Article

A Heterocyclic Peptide Nanotube

W. Seth Horne, C. David Stout, and M. Reza Ghadiri

J. Am. Chem. Soc., **2003**, 125 (31), 9372-9376• DOI: 10.1021/ja034358h • Publication Date (Web): 09 July 2003

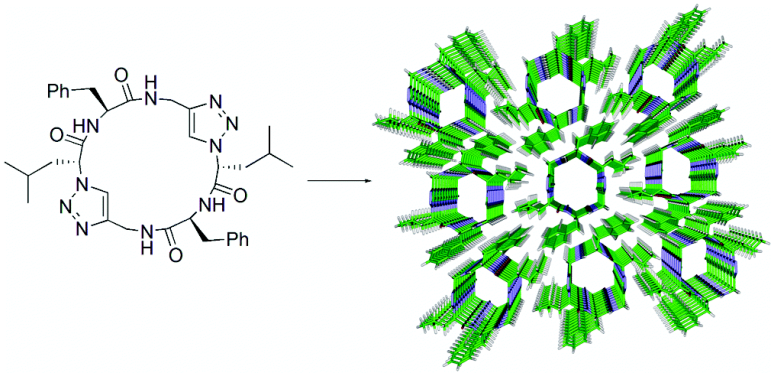

More About This Article

Additional resources and features associated with this article are available within the HTML version:

- Supporting Information
- Links to the 34 articles that cite this article, as of the time of this article download
- Access to high resolution figures
- Links to articles and content related to this article
- Copyright permission to reproduce figures and/or text from this article

View the Full Text HTML

J|A|C|S
ARTICLES
Published on Web 07/09/2003

A Heterocyclic Peptide Nanotube

W. Seth Horne, C. David Stout, and M. Reza Ghadiri*

Contribution from the Departments of Chemistry and Molecular Biology and The Skaggs Institute for Chemical Biology, The Scripps Research Institute, La Jolla, California 92037

Received January 27, 2003; E-mail: ghadiri@scripps.edu

Abstract: An open-ended hollow tubular structure is designed based on hydrogen-bond-directed self-assembly of a chimeric cyclic peptide subunit comprised of alternating α- and ϵ-amino acids. The design features a novel 1,4-disubstituted-1,2,3-triazole ϵ-amino acid and its utility as a peptide backbone substitute. The N-Fmoc-protected ϵ-amino acid was synthesized in high yield and optical purity in three steps from readily available starting materials and was employed in solid-phase peptide synthesis to afford the desired cyclic peptide structure. The cyclic peptide self-assembly has been studied in solution by ^{1}H NMR and mass spectrometry and the resulting tubular ensemble characterized in the solid state by X-ray crystallography.

Introduction

Organic tubular assemblies[1] constitute an expanding class of supramolecular structures with promising applications in chemical and biological settings.[2] Among various approaches developed for the construction of organic nanotubes, the hydrogen-bond-directed self-assembly of macrocyclic ring structures has proven particularly useful.[3] Specifically, self-assembling nanotubes have been designed based on cyclic peptides of alternating D,L-α-amino acids,[3a,b] β-amino acids,[3d,e] alternating α,β-amino acids,[3f] alternating α,γ-amino acids,[3g] δ-amino acids,[3h] and oligoureas.[3i,j] There are several advantages to the use of peptide-based macrocycles for nanotube assembly. Sequential condensation and deprotection of suitably protected amino acids provide a facile route for synthesis of the assembling subunits. The number and sequence of amino acids used defines the internal diameter and outside surface properties of the resulting tubular assembly. These design choices are not purely aesthetic, as it has been shown that the functional characteristics of such organic nanotubes depend on the nature of both their interior and their exterior surfaces.[2,4] The hydrophilic nature of the peptide nanotube interior has been an important feature in designing transmembrane ion channels and pores.[2,4] By contrast, peptide nanotubes possessing amphiphilic or hydrophobic internal characteristics have not yet been widely available due to the constraints imposed by the peptide backbone properties.[3g] Modification of the interior properties requires peptide main-chain replacements with hydrophobic moieties that do not adversely effect the conformational requirements of the subunit for self-assembly via intermolecular hydrogen bonding. Here we describe the utility of heterocyclic peptide backbone modifications in the design of a new form of self-assembling peptide nanotube that combines the structural aspects and capacity for outside surface functionalization of previously described cyclic D,L-α-peptide nanotubes with heterocyclic alterations introduced to modify the physical properties of the nanotube interior.

Results and Discussion

The macroheterocyclic peptide **1** employed in the present study was designed based on similar structural considerations that have been previously noted for the cyclic D,L-α-peptide nanotube analogues. An even number of amino acids with alternating Cα stereochemistry was employed to instill a preference for adoption of a flat ring conformation in solution. In this conformation the side chains are presented on the exterior of the macrocycle with the amide backbone oriented perpen-

(1) (a) Bong, D. T.; Clark, T. D.; Granja, J. R.; Ghadiri, M. R. *Angew. Chem., Int. Ed. Engl.* **2001**, *40*, 988−1011. (b) Ranganathan, D.; Lakshmi, C.; Haridas, V.; Gopikumar, M. *Pure Appl. Chem.* **2000**, *72*, 365−372. (c) Harada, A.; Li, J.; Kamachi, M. *Nature* **1993**, *364*, 516−18. (d) Venkataraman, D.; Lee, S.; Zhang, J.; Moore, J. S. *Nature* **1994**, *371*, 591−3. (e) Gattuso, G.; Menzer, S.; Nepogodiev, S. A.; Stoddart, J. F.; Williams, D. J. *Angew. Chem., Int. Ed. Engl.* **1997**, *36*, 1451−1454. (f) Nelson, J. C.; Saven, J. G.; Moore, J. S.; Wolynes, P. G. *Science* **1997**, *277*, 1793−1796. (g) Fenniri, H.; Mathivanan, P.; Vidale, K. L.; Sherman, D. M.; Hallenga, K.; Wood, K. V.; Stowell, J. G. *J. Am. Chem. Soc.* **2001**, *123*, 3854−3855.

(2) (a) Fernandez-Lopez, S.; Kim, H. S.; Choi, E. C.; Delgado, M.; Granja, J. R.; Khasanov, A.; Kraehenbuehl, K.; Long, G.; Weinberger, D. A.; Wilcoxen, K. M.; Ghadiri, M. R. *Nature* **2001**, *412*, 452−455. (b) Sanchez-Quesada, J.; Kim, H. S.; Ghadiri, M. R. *Angew. Chem., Int. Ed.* **2001**, *40*, 2503−2506. (c) Motesharei, K.; Ghadiri, M. R. *J. Am. Chem. Soc.* **1997**, *119*, 11306−11312.

(3) (a) Ghadiri, M. R.; Granja, J. R.; Milligan, R. A.; McRee, D. E.; Khazanovich, N. *Nature* **1993**, *366*, 324−327. (b) Hartgerink, J. D.; Granja, J. R.; Milligan, R. A.; Ghadiri, M. R. *J. Am. Chem. Soc.* **1996**, *118*, 43−50. (c) Clark, T. D.; Buriak, J. M.; Kobayashi, K.; Isler, M. P.; McRee, D. E.; Ghadiri, M. R. *J. Am. Chem. Soc.* **1998**, *120*, 8949−8962. (d) Seebach, D.; Matthews, J. L.; Meden, A.; Wessels, T.; Baerlocher, C.; McCusker, L. B. *Helv. Chim. Acta* **1997**, *80*, 173−182. (e) Clark, T. D.; Buehler, L. K.; Ghadiri, M. R. *J. Am. Chem. Soc.* **1998**, *120*, 651−656. (f) Karle, I. L.; Handa, B. K.; Hassall, C. H. *Acta Crystallogr., Sect. B* **1975**, *31*, 555−560. (g) Amorin, M.; Castedo, L.; Granja, J. R. *J. Am. Chem. Soc.* **2003**, *125*, 2844−2845. (h) Gauthier, D.; Baillargeon, P.; Drouin, M.; Dory, Y. L. *Angew. Chem., Int. Ed. Engl.* **2001**, *40*, 4635−4638. (i) Semetey, V.; Didierjean, C.; Briand, J. P.; Aubry, A.; Guichard, G. *Angew. Chem., Int. Ed. Engl.* **2002**, *41*, 1895−1898. (j) Ranganathan, D.; Lakshmi, C.; Karle, I. L. *J. Am. Chem. Soc.* **1999**, *121*, 6103−6107.

(4) (a) Granja, J. R.; Ghadiri, M. R. *J. Am. Chem. Soc.* **1994**, *116*, 10785−10786. (b) Sanchez-Quesada, J.; Isler, M. P.; Ghadiri, M. R. *J. Am. Chem. Soc.* **2002**, *124*, 10004−10005. (c) Engels, M.; Bashford, D.; Ghadiri, M. R. *J. Am. Chem. Soc.* **1995**, *117*, 9151−9158.

10.1021/ja034358h CCC: $25.00

Scheme 1

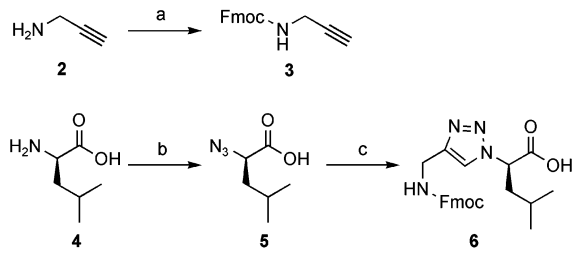

(a) Fmoc-*N*-hydroxysuccinimide (71%); (b) $(F_3CSO_2)_2O$, NaN_3, then $CuSO_4$, K_2CO_3 (84%); (c) **3**, CuI, diisopropylethylamine, 2,6-lutidine (97%).

dicular to the plane of the ring. This provides complementary hydrogen-bond donor and acceptor pairs on each face of the ring structure, enabling cyclic peptide self-assembly. Molecular modeling suggested that within this peptide framework the triazole backbone moiety could adopt a number of conformations that would be productive with respect to the intermolecular hydrogen-bond-directed stacking.

The required 1,2,3-triazole ϵ-amino acid precursor **6,** suitable for use in peptide synthesis, was readily synthesized in three steps from the corresponding optically pure free amino acid in 81% overall yield (Scheme 1). Commercially available propargylamine (**2**) was protected as the *N*-fluorenylmethylcarbamate (**3**) by treatment with Fmoc-NHS.[5] The free amino acid D-leucine (**4**) was converted to α-azido acid **5** by copper(II)-catalyzed diazo transfer from in-situ-generated triflyl azide.[6] Alkyne **3** and azide **5** in the presence of catalytic amounts of copper(I) and base underwent a rapid 1,3-dipolar cycloaddition reaction to afford triazole **6** in 97% isolated yield.[7] The synthesis of the triazole-backbone-modified linear peptide was performed on polystyrene solid support using the acid-labile trityl linker and Fmoc-phenylalanine as the first residue (Scheme 2). Solid-phase Fmoc peptide synthesis was carried out using standard protocols except for coupling of the triazole residues which were performed under base-free conditions to minimize racemization.[8] The linear peptide **8** was cleaved from the resin by treatment with 5% TFA/CH_2Cl_2 and purified by RP-HPLC (66% isolated yield). Exposure of the linear peptide in DMF to activating agents (PyBOP, HOAT, DIEA) resulted in a rapid macrolactamization yielding **1**. Pure peptide **1** was isolated in 65% yield after repeated trituration/crystallization from water/MeCN.

^{1}H NMR spectroscopy was employed to probe the aggregation propensity of **1** in solution. The spectrum in the polar solvent DMSO is sharp with well-resolved signals, while in the nonpolar solvent chloroform peaks broaden significantly (Figure 1). Moreover, ^{1}H NMR spectra in $CDCl_3$ display significant concentration-dependent chemical shifts. These observations are consistent with hydrogen-bond-mediated intermolecular aggregation giving rise to multiple supramolecular species in fast exchange on the NMR time scale. To approximate the equilibrium binding associations between interacting species in solution, ^{1}H NMR spectra in $CDCl_3$ at a range of concentrations

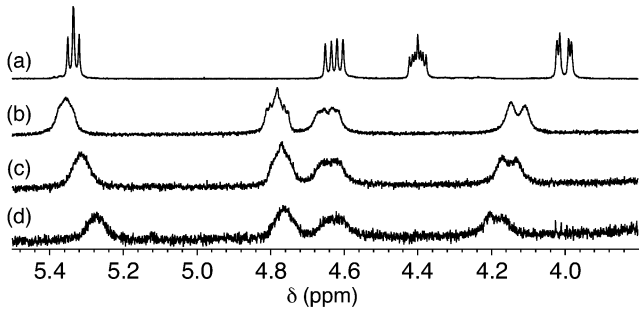

Figure 1. Selected region of ^{1}HNMR spectrum of **1** (a) in DMSO, (b) 1.0 mM in $CDCl_3$, (c) 0.50 mM in $CDCl_3$, and (d) 0.25 mM in $CDCl_3$. The peaks in DMSO show sharp splitting, while the signals in $CDCl_3$ are broad and show concentration-dependent chemical shifts.

from 1.0 mM to 63 μM were analyzed according to the model developed by LaPlanche et al.[9] to derive apparent association constants for formation of dimeric ($K_2 = 8.6 \times 10^4$ M^{-1}) and higher order aggregate species ($K_n = 3.8 \times 10^4$ M^{-1}). The apparent equilibrium constants correspond to 6.7 kcal·mol^{-1} driving force for peptide dimerization and 6.2 kcal·mol^{-1} for each subunit added to form a higher order aggregate. The aggregation propensity of peptide **1** was also evident by electrospray ionization mass spectrometry. Infusion of a 0.5 mM solution of **1** in 9:1 acetonitrile:water gave rise to strong signals corresponding to monomeric $[\mathbf{1}+H]^+$ (calcd = 683.4, obsd = 683.7), $[\mathbf{1}+Na]^+$ (calcd = 705.4, obsd = 705.7) as well as noncovalent dimers $[\mathbf{1}\cdot\mathbf{1}+H]^+$ (calcd = 1365.8, obsd = 1365.5) and $[\mathbf{1}\cdot\mathbf{1}+Na]^+$ (calcd = 1387.7, obsd = 1387.2).

X-ray crystallography was employed to elucidate the structural characteristics of **1** in the solid state. Small needlelike crystals with high aspect ratios were grown by slow evaporation from a saturated solution of **1** in ethanol and used to obtain X-ray diffraction data at −160 °C to 1.8 Å resolution. As direct methods are not applicable at this resolution, the crystal structure was solved using molecular replacement techniques and restrained refinement to give a structure with $R = 16.7\%$ ($R_{free} = 18\%$). The crystal structure (Figure 2) indicates that the peptide subunits adopt the expected flat ring shape conformation and stack in a parallel fashion into tubular assemblies with ordered ethanol molecules filling the channel pores. It is noteworthy to point out that the nanotube solid-state structure does not seem to be an artifact of the crystal packing forces as a single cyclic peptide comprises the contents of the unit cell (P1). The triazole rings orient perpendicular to the overall macrocycle, lining the nanotube interior with π electron-rich heteroaromatic moieties. Three of the four amide bonds in the ring backbone form a network of intermolecular hydrogen bonds with N−O distances of 3.3 Å.[10] The remaining amide bond is involved in an apparent ethanol-mediated bridging hydrogen bond with N−O and O−O distances of 2.7 Å. The portion of the amide backbone involved in this bridging hydrogen bond is slightly tilted, relative to the rest of the ring, with the amide N−H pointing more toward the ethanol oxygen than along the tube axis. The peptide nanotube channel is roughly oval in shape with internal van der Waals diameter ranging from 5.2 Å between the triazole rings to 6.8

(5) Tong, G.; Lawlor, J. M.; Tregear, G. W.; Haralambidis, J. *J. Org. Chem.* **1993**, *58*, 2223−2231.
(6) (a) Alper, P. B.; Hung, S.-C.; Wong, C.-H. *Tetrahedron Lett.* **1996**, *37*, 6029−6032. (b) Lundquist IV, J. T.; Pelletier, J. C. *Org Lett.* **2001**, *3*, 781−783.
(7) (a) Rostovtsev, V. V.; Green, L. G.; Fokin, V. V.; Sharpless, K. B. *Angew. Chem., Int. Ed. Engl.* **2002**, *41*, 2596−2599. (b) Tornøe, C. W.; Christensen, C.; Meldal, M. *J. Org. Chem.* **2002**, *67*, 3057−3064.
(8) Coupling reactions of **6** in the presence of diisopropylethylamine led to substantial racemization at the stereocenter adjacent to the triazole.
(9) LaPlanche, L. A.; Thompson, H. B.; Rogers, M. T. *J. Phys. Chem.* **1965**, *69*, 1482−1488.
(10) For a review of hydrogen bonding, see: G. A. Jeffrey. *An Introduction to Hydrogen Bonding*; Oxford University Press: New York, 1997.

Scheme 2

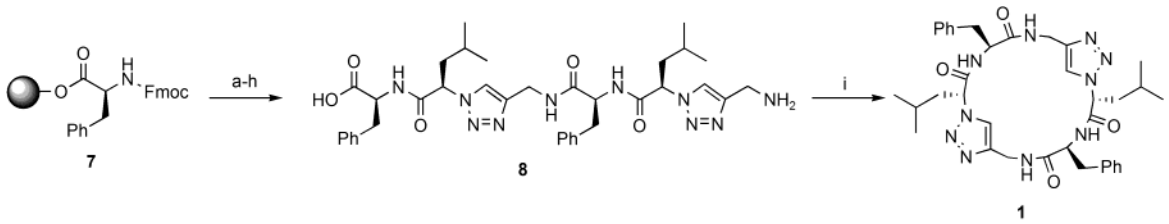

(a) 20% piperidine/DMF; (b) **6**, DIC, HOBT; (c) 20% piperidine/DMF; (d) Fmoc-Phe-OH, HBTU, DIEA; (e) 20% piperidine/DMF; (f) **6**, DIC, HOBT; (g) 20% piperidine/DMF; (h) 5% TFA/DCM; (i) PyBOP, HOAT, DIEA.

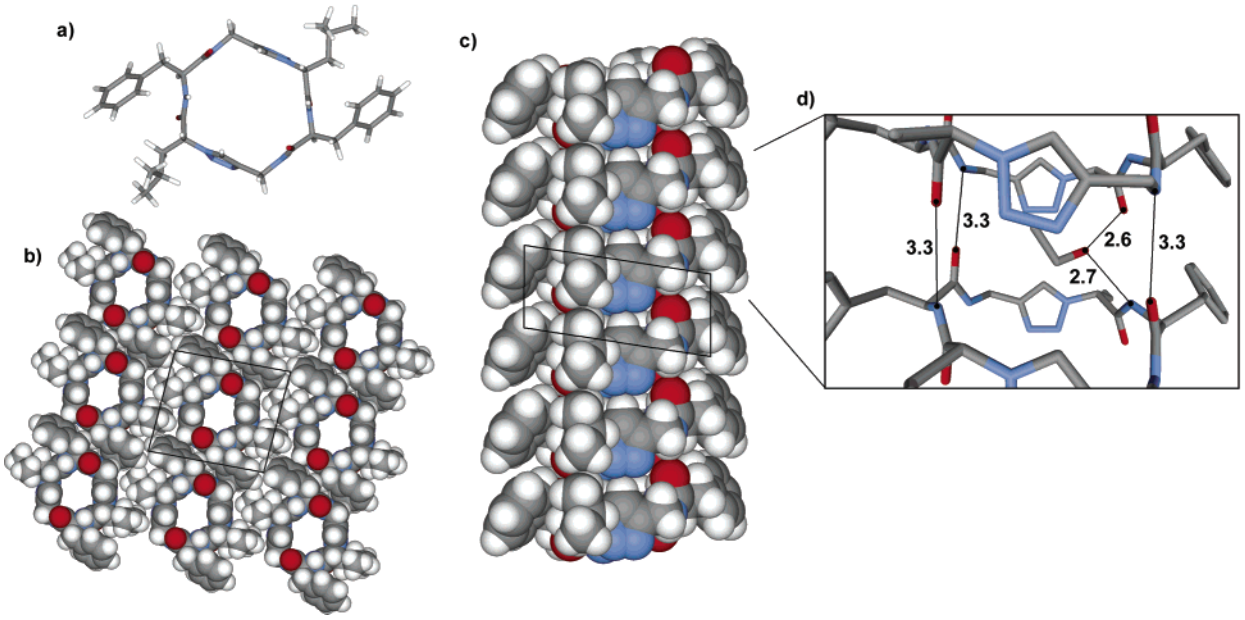

Figure 2. Crystal structure of **1**: (a) single molecule viewed from the top (solvent omitted), (b) crystal packing viewed along the tube axis (solvent omitted), (c) one tube viewed from the side (solvent omitted), and (d) expanded view of the interaction between two rings with heteroatom−heteroatom distances for indicated hydrogen-bonding moieties labeled in Å (protons omitted).

Å between the phenylalanine α carbons. Volume calculations[11] suggest an approximately 80 Å^3 cavity size per macrocycle repeat along the tube axis with the ethanol filling about 60% of this space.[12]

Conclusion

We have described the design, synthesis, and characterization of a new class of peptide-based macrocycle incorporating 1,2,3-triazole ϵ-amino acids in the backbone. The synthesis is modular and straightforward with the protected triazole ϵ-amino acid readily prepared from the corresponding free amino acid. In the solid state, these molecules form a solvent-filled nanotube held together by an extended network of intermolecular amide backbone hydrogen bonds. NMR and mass spectrometry studies support similar behavior in solution and the gas phase.

Experimental Section

General. 2-(1*H*-benzotriazole-1-yl)-1,1,3,3-tetramethyluronium hexafluorophosphate (HBTU), benzotriazole-1-yl-oxy-tris-pyrrolidino-phosphonium hexafluorophosphate (PyBOP), Fmoc-phenylalanine, leucine, and trityl chloride resin were purchased from Novabiochem. Trifluoromethanesulfonic anhydride was purchased from Lancaster. All other reagents were purchased from Aldrich or Fisher. All reagents and solvents were used as received unless otherwise noted. All NMR spectra were obtained on a Varian Inova-400 MHz or Bruker AMX-500 MHz spectrometer. Electrospray ionization mass spectrometry infusion experiments were carried out on Hitachi M-8000 ion trap and Agilent 1100 quadrapole mass spectrometers.

Prop-2-ynyl-carbamic acid, 9H-fluoren-9-ylmethyl ester (3).[5] Fmoc-*N*-hydroxysuccinimide (2.0 g, 5.9 mmol) was suspended in THF (12 mL). The solution was cooled on an ice bath, and propargylamine (0.427 mL, 6.23 mmol) was added dropwise. The reaction was stirred and allowed to warm to room temperature over 2 h. The THF was removed under vacuum. The residue was dissolved in EtOAc (150 mL) and washed with water (3 × 50 mL). The organic layer was dried and concentrated. The crude solid was recrystallized from EtOAc to yield 1.164 g (71%) of the desired product as white needles. ^{1}H NMR (500 MHz, DMSO-d_6) δ 7.88 (d, J = 8 Hz, 2H), 7.78 (t, J = 6 Hz, 1H), 7.68 (d, J = 7 Hz, 2H), 7.41 (t, J = 7 Hz, 2H), 7.32 (dt, J = 1, 7 Hz, 2H), 4.31 (d, J = 7 Hz, 2H), 4.21 (t, J = 7 Hz, 1H), 3.77 (dd, J = 2, 6 Hz, 2H), 3.10 (t, J = 2 Hz, 1H); ^{13}C NMR (125 MHz, DMSO-d_6) δ 155.9, 143.8, 140.7, 127.6, 127.1, 125.2, 120.1, 81.4, 73.1, 65.7, 46.6, 29.8; ESI-MS (m/z) 278 [M+H]$^+$ (MW$_{calcd}$ = 277).

2-(R)-{4-[(9H-Fluoren-9-ylmethoxycarbonylamino)-methyl]-[1,2,3]-triazol-1-yl}-4-methyl-pentanoic acid (6). Azido-D-leucine[6b] (**5**) (157 mg, 1.0 mmol) and Fmoc-propargylamine (**3**) (277 mg, 1.0 mmol) were dissolved in degassed acetonitrile (4 mL). To this solution, 2,6-lutidine (0.233 mL, 2.0 mmol) and diisopropylethylamine (0.348 mL, 2.0 mmol) were added under Ar. Copper(I) iodide (19 mg, 0.1 mmol) was then added to the solution. The reaction was stirred under Ar for 3 h. Most

(11) Volume calculations were carried out using GRASP: Nicholls, A.; Sharp, K. A.; Honig, B. *Proteins* **1991**, *11*, 281−296.
(12) This observation is consistent with a study suggesting 0.55 ± 0.09 as the ideal packing coefficient for guests in supramolecular systems: Mecozzi, S.; Rebek, J., Jr. *Chem. Eur. J.* **1998**, *4*, 1016−1022.

Table 1. Concentration-Dependent ^{1}H NMR Chemical Shifts

signal	δ at 1.0 mM (Hz)	δ at 0.50 mM (Hz)	δ at 0.25 mM (Hz)	δ at 0.125 mM (Hz)	δ at 0.0625 mM (Hz)
Leu ϵ CH_3	292	296	300	303	308
Leu γ CH	378	387	399	408	*a*
Leu β CH_2 (1)	772	777	781	788	*a*
Phe β CH_2 (1)	1233	1226	1222	1219	*a*
backbone CH_2 (1)	1650	1659	1673	1683	1706
backbone CH_2 (2)	1857	1854	1849	1841	1831
Phe α CH	1911	1907	1904	1901	1899
Leu α CH	2141	2124	2107	2087	2059
amide NH (1)	3212	3147	3086	*a*	*a*

[a] Signal was either buried under another peak or not visible above noise at the lowest concentration acquisition.

of the MeCN was removed under vacuum, and the resulting residue was dissolved in EtOAc (150 mL). The solution was washed with 9:1 satd NH_4Cl:NH_4OH and then twice with 0.5 N HCl. The organic phase was dried and concentrated to yield 420 mg (97%) of the desired product as a white solid, which was used without further purification. An analytically pure sample was obtained by recrystallization from hot EtOAc/hexanes. $[\alpha]^{22}_D = -8.9$ ($c = 10$ mg/mL in $CHCl_3$); ^{1}H NMR (500 MHz, DMSO-d_6) δ 8.00 (s, 1H), 7.88 (d, $J = 7$ Hz and s, total 3H), 7.69 (d, $J = 7$ Hz, 2H), 7.40 (t, $J = 7$ Hz, 2H), 7.31 (t, $J = 7$ Hz, 2H), 5.39 (dd, $J = 4$, 11 Hz, 1H), 4.4−4.2 (m, 3H), 3.7−3.1 (broad s, 1H), 2.2−2.1 (m, 1H), 2.0−1.8 (m, 1H), 1.2−1.1 (m, 1H), 0.83 (dd, $J = 7$, 23 Hz, 6H); ^{13}C NMR (125 MHz, DMSO-d_6) δ 170.7, 156.2, 145.0, 143.9, 140.7, 127.6, 127.1, 125.2, 122.6, 120.1, 65.6, 60.5, 46.7, 36.0, 24.3, 22.6, 20.9 (signal for methylene carbon on isobutyl side chain is buried under solvent peaks ~39 ppm and was identified by a cross-peak observed in an HMQC experiment); ESI-MS (*m*/*z*) 435.2 $[M+H]^+$ ($MW_{calcd} = 434.2$).

Linear Peptide 8. (a) Loading of resin: Fmoc-phenylalanine (482 mg, 1.245 mmol) and diisopropylethylamine (0.217 mL, 1.245 mmol) were dissolved in CH_2Cl_2 (5 mL) and added to trityl chloride resin (500 mg, 1.66 mmol/g max loading). The mixture was agitated on a shaker for 4 h. The vessel was then drained, and the resin was washed with 8:2:1 CH_2Cl_2:MeOH:DIEA (2 × 10 min), CH_2Cl_2 (3 × 1 min), and Et_2O. After drying under vacuum, loading was quantified by UV quantitation of Fmoc release. Final loading was found to be 1.0 mmol/g.

(b) Peptide Synthesis: The resin (150 mg, 0.100 mmol) prepared above was placed in a sintered glass peptide synthesis vessel and swollen in CH_2Cl_2 for 45 min. The resin was washed twice with DMF, treated with 20% piperidine/DMF (2 × 8 min) to remove the Fmoc group, and washed again with DMF (3×). A solution of **6** (241 mg, 0.555 mmol), diisopropylcarbodiimide (70 mg, 0.555 mmol), and HOBT·H_2O (85 mg, 0.555 mmol) in DMF (2 mL) was added to the vessel. The resin suspension was agitated for 30 min, drained, and washed with DMF (3×). After Fmoc deprotection and washing as above, a solution of Fmoc-phenylalanine (233 mg, 0.602 mmol), HBTU (210 mg, 0.553 mmol), and diispropylethylamine (0.263 mL, 1.501 mmol) in DMF (2 mL) was added. The coupling was carried out for 30 min followed by washing and Fmoc deprotection. The final coupling of **6** was carried out under the same conditions as the first coupling. After removal of the terminal Fmoc, the resin was washed with DMF (3×) and then CH_2Cl_2 (3×). Product was cleaved from the resin by treatment with 5% TFA in CH_2Cl_2 (5 × 3 mL) followed by washing with CH_2Cl_2 and MeOH. The acid solution and subsequent washes were combined and concentrated under vacuum. Water was added to the oily residue, and the resulting suspension was frozen and lyophilized. The crude product was purified by preparative reverse-phase HPLC on a C_{18} column to yield 46 mg of **8** (66% based on resin loading). MALDI−FTMS (*m*/*z*) 701.3886 $[M+H]^+$ ($MW_{calcd} = 701.3882$).

Macrocycle 1. Linear precursor **8** (29 mg, 0.041 mmol) was dissolved in DMF (29 mL). PyBOP (32 mg, 0.061 mmol), HOAT (0.123 mL of 0.5 M solution in DMF, 0.061 mmol), and DIEA (0.043 mL, 0.245 mmol) were added to the solution. After stirring for 90 min, the DMF was removed under vacuum. The resulting residue was triturated with 4:1 water:acetonitrile (3 × 10 mL). The remaining solid was dried under vacuum to yield 18 mg (65%) of **1**. ^{1}H NMR (500 MHz, DMSO-d_6) δ 9.06 (d, $J = 7$ Hz, 2H), 8.66 (dd, $J = 4$, 8 Hz, 2H), 7.91 (s, 2H), 7.32−7.26 (m, 8H), 7.24−7.18 (m, 2H), 5.33 (t, $J = 7$ Hz, 2H), 4.63 (dd, $J = 8$, 16 Hz, 2H), 4.45−4.35 (m, 2H), 4.00 (dd, $J = 4$, 16 Hz, 2H), 3.00 (dd, $J = 4$, 14 Hz, 2H), 2.77 (dd, $J = 11$, 14 Hz, 2H), 1.6−1.5 (m, 2H), 1.5−1.4 (m, 2H), 0.9−0.8, (m, 2H), 0.70 (t, $J = 7$ Hz, 12H); ^{13}C NMR (125 MHz, DMSO-d_6) δ 170.9, 167.7, 146.1, 137.7, 129.1, 128.1, 126.4, 120.4, 60.5, 55.4, 43.1, 37.0, 34.4, 24.0, 22.1, 21.8; MALDI−FTMS (*m*/*z*) 683.3774 $[M+H]^+$ ($MW_{calcd} = 683.3776$).

Crystal Data Collection and Structure Determination. Crystals of **1** were prepared by slow evaporation of a saturated in solution in ethanol. Each crystal was mounted on a cryo-loop with paratone-N oil. Data were collected on an Raxis IV image plate detector equipped with Osmic confocal mirrors and Xstream cryo-device (100K) using Cu Kα radiation ($\lambda = 1.5418$ Å) from a Ru200 X-ray generator operated at 50 kV, 100 mA. Data were processed using MSC Crystal Clear. The space group was determined to be *P*1 with cell dimensions $a = 5.51$ Å, $b = 12.59$ Å, $c = 14.71$ Å, $\alpha = 83.30°$, $\beta = 72.61°$, $\gamma = 81.88°$. The data set was 96% complete and included 2356 reflections of which 320 were unique. The scaling and averaging gave an R_{merge} of 7.4%. The mean I/σ was 6.7, and the average multiplicity for the data set was 7.3. Each cell contains **1**·EtOH ($C_{36}H_{46}N_{10}O_4$·C_2H_6O).

The structure was solved by molecular replacement and restrained refinement using the CCP4 program suite.[13] The search model was generated from an energy-minimized structure of **1** calculated in the Discover module of InsightII. Geometric restraints for the triazole portion were assembled from a survey of 1,4-disubstituted 1,2,3-triazoles in the Cambridge Structural Database. Hydrogen atoms were used in the refinement but were fixed to moving C, N, and O atoms. After several cycles of restrained refinement, electron density for the ethanol was located in a $|F_o| - |F_c|$ map and modeled. The final model gave an R_{factor} of 16.7% for all data and an R_{free} value of 18.0% for 10% of the data set aside throughout structure solution and refinement. The mean *B* value for the model was 17.8 Å^2 with rms deviations from ideal bond lengths and angles of 0.02 Å and 2.6°, respectively.

Variable-Concentration ^{1}H NMR. A 1.0 mM stock solution of **1** was prepared in $CDCl_3$. Serial 2-fold dilutions were carried out to produce 0.5, 0.25, 0.125, and 0.0625 mM stocks. A 0.6 mL amount of each solution was transferred to separate NMR tubes. These tubes were placed on an autosampler, and ^{1}HNMR spectra were acquired on a Varian 400 MHz instrument. As all peaks are broad, each chemical shift was recorded as the midpoint of the observed signal. The recorded data is summarized in Table 1.

(13) Software used in structure solution: (a) CCP4: Collaborative Computational Project Number 4. *Acta Crystallogr.* **1994**, *D50*, 760−763. (b) Xtalview: McRee, D. E. *J. Mol. Graphics* **1992**, *10*, 44−46.

Derivation of Apparent Equilibrium Constants. Using the model developed by LaPlanche et al.,[9] association constants were determined for the initial dimerization and higher order aggregation.

$$2\mathrm{A} \overset{K_2}{\rightleftharpoons} \mathrm{A}_2 \tag{1}$$

$$\mathrm{A}_{n-1} + \mathrm{A} \overset{K_n}{\rightleftharpoons} \mathrm{A}_n,\ n > 2 \tag{2}$$

In the above expressions, A represents peptide monomer and A_n represents n peptide monomers in a hydrogen-bonded assembly. In brief, the simplifying assumptions used in the modeling are (1) the monomer−dimer equilibrium has a unique binding constant K_2, (2) the association constants K_n for higher order aggregation events are all equal, (3) the chemical shift of a proton in assembly A_n does not depend on n when $n \geq 2$, (4) $[A_n] < [A_{n-1}]$ for $n > 2$, and (5) the amount of hydrogen bonding by the solvent is negligible. Also, although **1** exhibited parallel stacking in the solid state, antiparallel stacking is also possible. To reduce calculations to a manageable level, antiparallel species were not included.

From the equations derived by LaPlanche,[9] the chemical shift δ_{calcd} for a given proton in the above system satisfies

$$\delta_{calcd} = (\delta_1 - \delta_n)x + \delta_n \tag{3}$$

$$x = \left[\frac{1 + \dfrac{K_2 A_1}{1 - K_n A_1}}{1 + \dfrac{K_2 A_1 (2 - K_n A_1)}{(1 - K_n A_1)^2}} \right] \tag{4}$$

where A_1 represents the mole fraction of free monomer in solution, δ_1 is the chemical shift of the proton in the monomer, and δ_n is the chemical shift in aggregate species. A_1 for given values of C, K_2, and K_n is found by solving the root of

$$[K_n^2(C+1) - K_n K_2 C - K_n K_2]A_1^3 + [-2K_n(C+1) - K_n^2 C + K_2 C + 2K_2]A_1^2 + [(C+1) + 2K_n C]A_1 - C = 0 \tag{5}$$

where C is defined as the fraction of moles of total peptide added to moles of solvent. As eq 5 has only one real root subject to the physical constraints of the experiment, an A_1 value for a given pair of K_2 and K_n can be determined explicitly for any experimental concentration. Thus, experimental $\{\delta_{obsd}, C\}$ pairs for a given signal in the NMR spectrum can be used eq 3 to find corresponding δ_1 and δ_n by linear regression analysis.

K_2 and K_n were used as parameters in the above model to fit δ_{obsd} measured for nine protons in **1** at five concentrations in $CDCl_3$. The objective function was defined as the sum of the squares of the residuals between δ_{calcd} and δ_{obsd} for all signals. Nonlinear numerical minimization algorithms were used to find the K_2 and K_n values showing the best overall agreement with experimental data.

Acknowledgment. We thank the National Institute of General Medical Sciences (GM52190) for financial support, Professor K. B. Sharpless for valuable discussions, and the NSF for a predoctoral fellowship to S.H.

Supporting Information Available: Atomic coordinates for **1** (CIF format). This material is available free of charge via the Internet at http://pubs.acs.org. See any current masthead page for ordering information and Web access instructions.

JA034358H